Thermally driven hydrogen interaction with single-layer graphene on SiO$_2$/Si substrates quantified by isotopic labeling

(iD) Taís Orestes Feijó, (iD) Guilherme Koszeniewski Rolim, (iD) Silma Alberton Corrêa, (iD) Cláudio Radtke, and (iD) Gabriel Vieira Soares

View Online   Export Citation   CrossMark

ARTICLES YOU MAY BE INTERESTED IN

Thermally driven hydrogen interaction with single-layer graphene on SiO₂/Si substrates quantified by isotopic labeling

Taís Orestes Feijó,[1] (ID) Guilherme Koszeniewski Rolim,[1] (ID) Silma Alberton Corrêa,[2] (ID) Cláudio Radtke,[2] (ID) and Gabriel Vieira Soares[3,a] (ID)

AFFILIATIONS

[1]Programa de Pós-Graduação em Microeletrônica, UFRGS, 91501-970 Porto Alegre, RS, Brazil
[2]Instituto de Química, UFRGS, 91501-970 Porto Alegre, RS, Brazil
[3]Instituto de Física, UFRGS, 91501-970 Porto Alegre, RS, Brazil

[a]Author to whom correspondence should be addressed: gabriel.soares@ufrgs.br

ABSTRACT

In the present work, we investigated the interaction of hydrogen with single-layer graphene. Fully hydrogenated monolayer graphene was predicted to be a semiconductor with a bandgap of 3.5 eV in contrast to the metallic behavior of its pristine counterpart. Integration of these materials is a promising approach to develop new electronic devices. Amidst numerous theoretical works evidencing the efficient formation of fully hydrogenated graphene, few experimental studies have tackled this issue. A possible explanation for that is the difficulty to directly quantify hydrogen by usual characterization techniques. Using an isotopically enriched gas in deuterium in conjunction with nuclear reaction analysis, we were able to quantify deuterium deliberately incorporated in graphene as a result of thermal annealing. The highest D areal density obtained following annealing at 800 °C was 3.5×10^{14} D/cm². This amount corresponds to ~10% of the carbon atoms in graphene. Spectroscopic results evidence that deuterium is predominantly incorporated in grain boundaries accompanied by rippling and etching of graphene, the latter effect being more pronounced at higher temperatures. Desorption experiments show that hydrogen (deuterium) incorporation is not completely reversible due to the damage induced in the graphene layer through the hydrogen adsorption/desorption cycle.

INTRODUCTION

Graphene was synthesized for the first time in 2004, by Andre Geim and Konstantin Novoselov, using micromechanical exfoliation of graphite.[1–3] Since then, several strategies were developed to produce this material more efficiently. Obtaining graphene with good quality in large areas is of fundamental importance. Chemical vapor deposition (CVD),[4] silicon sublimation from silicon carbide,[5] and molecular beam epitaxy (MBE)[6] are some of the techniques used for this goal. High-quality graphene on wafers was already obtained by the roll-to-roll method through CVD.[7] High performance graphene field-effect transistors have also been fabricated on a 2-in. SiC wafer evidencing the high quality of epitaxial graphene.[8]

These techniques include high temperature processing steps under different atmospheres. In the case of CVD, graphene transfer to suitable substrates is an additional mandatory step to fully exploit its properties. During the whole processing history of a graphene layer, it interacts with several gases at different temperatures. Hence, it is of fundamental importance to understand its interaction with different molecules to control manufacturing processes. Even in a clean room environment, the manufacture of electronic devices at high temperatures can induce unwanted modifications in graphene. For instance, annealing in vacuum followed by air exposure induces a high doping effect on graphene due to the adsorption of H_2O and O_2.[9] Moreover, chemisorption of hydrogen in graphene can lead to changes in the magnetic moment, modifying its electrical and magnetic properties, which are essential for electronic devices.[10] In contrast to undesirable effects induced by hydrogen, incorporation of this element in graphene can be used to intentionally modify its properties. A monolayer of fully

hydrogenated graphene is called graphane, which was predicted to be a semiconductor with a gap of 3.5 eV.[11] The integration of graphene with this semiconductor material is a promising approach to develop new electronic devices.[12]

Graphene may also be used for hydrogen storage in clean energy technologies. A monolayer of graphene without defects is expected to store a maximum of 7.7 wt. % hydrogen, which is more that can be stored with traditional methods in fuel cells.[11] A theoretical structure where graphene layers kept at a fixed distance by carbon nanotubes pillars was predicted to have a hydrogen storage capacity of 6 wt. %.[13] Another efficient method for high-density hydrogen storage has been proposed through the intercalation of molecular hydrogen in graphane nanofibers (17 wt. %).[14] Graphane functionalized with OLi_2 also proved to be a potential hydrogen storage material, with the storage capacity being able to reach 12.9 wt. %.[15]

Amidst numerous theoretical works evidencing the efficient formation of fully hydrogenated graphene, few experimental studies have tackled this issue. A possible explanation for that is the difficulty to directly quantify hydrogen by usual characterization techniques. Luo *et al.* investigated the evolution of hydrogenated graphene electronic structures using XPS to evaluate hydrogen incorporation. H coverage is defined through the intensity ratio of sp^3 to sp^2-hybridized carbon components.[16] Burgess *et al.* also investigated the extent of hydrogenation of graphene treated in a plasma reactor using Raman spectroscopy.[17] Both techniques are based on the investigation of modifications induced by hydrogenation in the graphene layer, constituting indirect methods of its actual quantification. Thus, they are susceptible to several interferences such as undeliberate hydrogen incorporation by sample contamination, for example.

In this scenario, it is crucial to understand how hydrogen interacts with graphene in specific processing conditions. Such knowledge includes quantification of incorporated hydrogen during graphene processing in high temperatures and possible modifications in the graphene layer induced by these processes. In the present work, we investigated hydrogen incorporation and desorption in graphene monolayers upon thermal annealing. We used a hydrogen atmosphere isotopically enriched in deuterium. Nuclear reaction analysis (NRA) was used to quantify the deuterium amount incorporated in these samples with isotopic specificity, enabling the determination of the areal density of hydrogen (deuterium) deliberately incorporated in graphene as a result of thermal annealing. Spectroscopic techniques were also employed to follow structural and compositional modifications of the graphene layer.

EXPERIMENTAL PROCEDURE

Monolayer graphene samples grown by chemical vapor deposition on copper and then transferred on 285 nm of SiO_2 on Si were purchased from Graphene Supermarket™. SiO_2/Si samples without graphene were used for comparison. The sample size was 5×10 mm. A static pressure and resistively heated quartz tube furnace was used, which was initially pumped down to 2×10^{-7} mbar. Samples were annealed at 200 °C in vacuum to remove surface contaminants. After that, they were annealed for 60 min in a 1000 mbar H_2 atmosphere enriched to 99.8% in the deuterium

($^2H_2{=}D_2$) rare isotope. The temperature of this last step was in the 200–800 °C range. This rare isotope (0.015% natural abundance) was chosen in order to evaluate H incorporation specifically due to the annealing step. To investigate hydrogen desorption from graphene, samples underwent an annealing step in a D_2 atmosphere for 60 min at 600 °C followed by an additional annealing in a nitrogen (N_2) atmosphere for 60 min at temperatures ranging from 200 up to 800 °C. D quantification was accomplished by nuclear reaction analysis (NRA), using the $^3He(^2H_2,p)^4He$ nuclear reaction at 700 keV (10^{12} D/cm^2 sensitivity and 10% accuracy)[18] using an $^3He^+$ beam. The beam spot (diameter of ∼1 mm) was moved to different points on the sample surface after each spectrum acquisition aiming at keeping sample integrity. The products of the nuclear reaction are a proton (with an energy of 13 MeV) and a nucleus of ^4He (with an energy of 2 MeV). The detection of the former particles enables the quantification of hydrogen with D isotopic selectivity. Structural properties of graphene were accessed by Raman spectroscopy using the 482.5 nm line of a Kr^+ ion laser. High-resolution XPS and Near-Edge X-ray Absorption Fine Structure (NEXAFS) measurements were performed at the Brazilian Synchrotron Light Laboratory, Campinas, Brazil. The PGM (Planar Grating Monochromator) beamline, which is dedicated for x-ray spectroscopy in the soft x rays (100–1500 eV) and gives a spectral resolution (E/ΔE) from 1000 up to 25 000, was used as the monochromatic photon source. The beam spot on the sample (diameter of ∼1 mm) was moved to different points on the sample surface after each spectrum acquisition.

RESULTS

Figure 1 shows D areal densities as a function of the annealing temperature in D_2 atmosphere. Samples with (red circles) and

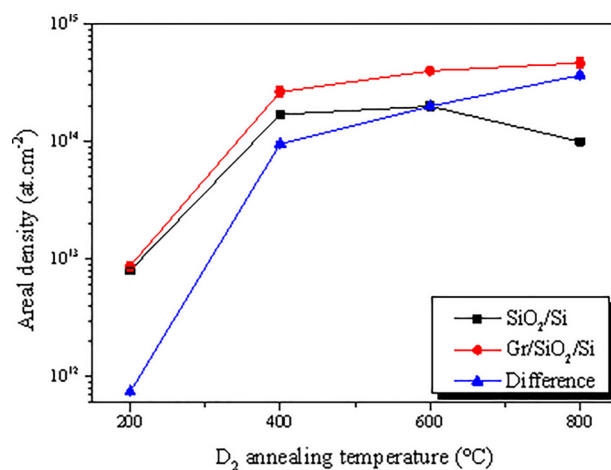**FIG. 1.** D areal densities as a function of D_2 annealing temperature for 285 nm thick SiO_2 films grown on Si (black squares) and single-layer graphene (SLG) transferred to 285 nm thick SiO_2 films grown on Si (red circles). The difference between D areal densities in samples with and without graphene is represented by blue triangles. Lines are only to guide the eyes.

without (black squares) graphene were annealed under the same conditions for comparison. The difference between D areal densities incorporated in these two sets of samples (blue triangles) represents the amount incorporated in graphene. At 200 °C, D incorporation was similar for both samples. The difference between both was below the sensitivity of the technique. At 400 °C, we observe a higher D incorporation in both samples, with a significant amount of samples with graphene. We observe a D incorporation of 1.0×10^{14} D/cm^2 only in graphene (triangles). At 600 °C, this amount increased to 2.0×10^{14} D/cm^2. At 800 °C, a 3.5×10^{14} D/cm^2 amount is reached. Considering the areal density of carbon atoms in graphene to be 3.82×10^{15} C/cm^2,[19] the maximum D incorporation of the present work corresponds to ~10% of this density. It is worth mentioning that this percentage is probably underestimated. The C areal density was calculated for a perfect graphene crystal, while CVD graphene presents defects and grain boundaries. Wang *et al.* used isotopic labeling to quantify the percentage of ^{13}C in the grain boundaries of graphene relative to the area of the graphene crystals grown with ^{12}C by CVD. They concluded that the percentage of carbon forming graphene grain boundaries is 5%–27% depending on the growth time.[20] Therefore, deuterium incorporation is probably taking place at graphene grain boundaries in our experiments.

X-ray photoelectron spectroscopy was used to determine the chemical modifications of graphene. Figure 2 shows C 1 s regions of photoelectron spectra obtained from samples (a) before annealing and those annealed in D$_2$ atmosphere at (b) 400 and (c) 600 °C. Figure 2(a) shows three bonding configurations in the pristine sample: sp^2-hybridized carbon in graphene at 284.6 eV, sp^3-hybridized carbon at 285.3 eV, and oxidized carbon at 286.5 eV.[21] Graphene grown on copper by CVD presents a sp^3-hybridized carbon component due to the adsorption of CH$_4$ during growth.[16] Furthermore, hydrocarbon and carboxyl PMMA functional groups used in the transfer step may also contribute to the increase of this component.[22] Air exposure prior to XPS measurements may also result in the appearance of contaminants.

Figure 2(b) shows that annealing in D$_2$ at 400 °C decreases the C—O component, evidencing the effects of thermal treatments in such a reducing atmosphere. Pristine samples were vacuum annealed and exposed to the air before XPS measurements, which may have led to the incorporation of air contaminants, such as CO$_x$ and O$_2$.[23] Air exposure took place each time before XPS analyses due to the sample transfer procedure between the annealing chamber and the load-lock from the XPS station. D$_2$ annealings were carried out in the same chamber of the vacuum pretreatment (*in situ*), drastically reducing the contribution of the C—O component in the spectrum. This fact indicates that the deuterium treatment passivated sites for contaminant incorporation.

Figure 2(c) shows that the increase in the D$_2$ annealing temperature decreases the sp^3-hybridized carbon component to 9.5% of the C 1 s signal. This percentage is comparable to that of carbon atoms possibly presenting a bond with deuterium. The amount of the latter incorporated at this annealing temperature was obtained by NRA, corresponding to 5.2% of C atoms in graphene (theoretical value). The decrease of the sp^3-hybridized carbon component with the D$_2$ annealing temperature can also be explained by
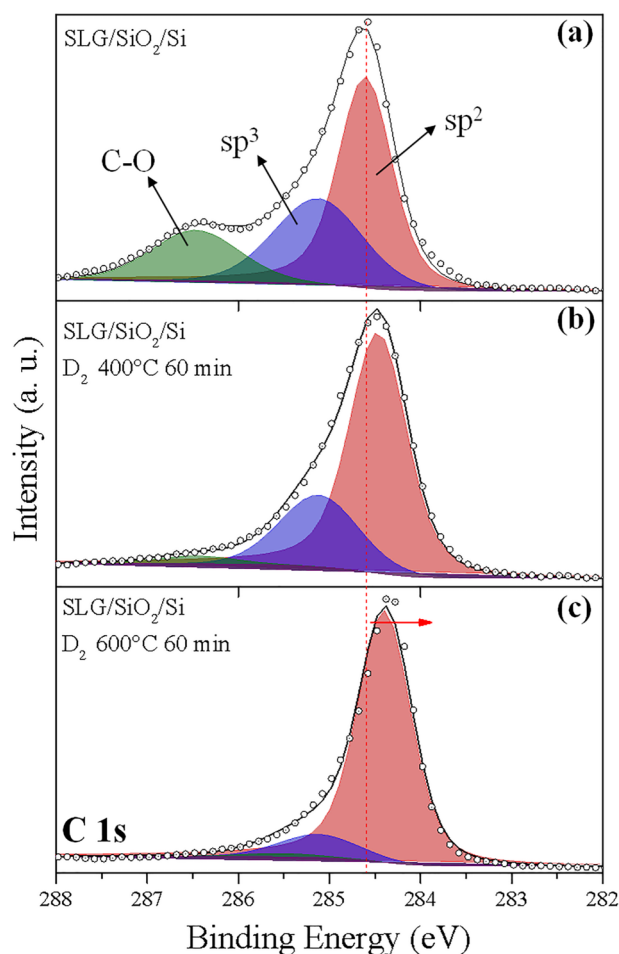

FIG. 2. XPS spectra of the (a) pristine sample and the sample annealed in D$_2$ at (b) 400 °C and (c) 600 °C. Deconvolution of the C 1 s region shows components sp^2 (orange), sp^3 (blue), and C—O (green).

removal of the air contaminants, bond healing in the basal plane of graphene, and increase of π delocalized electrons.[24]

Furthermore, we observed a shift of the sp^2-hybridized carbon component to lower binding energies with increasing D$_2$ annealing temperatures. This component shifts to a binding energy of 284.3 eV following D$_2$ annealing at 600 °C. This effect can be explained by graphene hydrogenation. Oxidation of carbon leads to a shift of the C 1 s components to higher binding energies.[25] Thus, the opposite effect is expected following reduction.

The Near-edge X-ray absorption fine structure (NEXAFS) was used to identify the orientation of carbon bonds for samples annealed in D$_2$. NEXAFS spectroscopy consists of the use of x rays to promote electrons from core levels to unoccupied states. Depending on the final state involved in the transition, π* and σ* type resonances can be distinguished. The directional properties of these resonances depend upon the molecular orientation in relation

to the electric-field vector of the synchrotron radiation.[26] We used two different angles of incidence. The angle of 26° (the angle between the sample surface and the direction of incidence) provides information of bonds pointing outside the sample plane (C 1 s → π* transitions), while an angle of 90°, information of bonds in the plane of the sample (C 1 s → σ* transitions).[26,27]
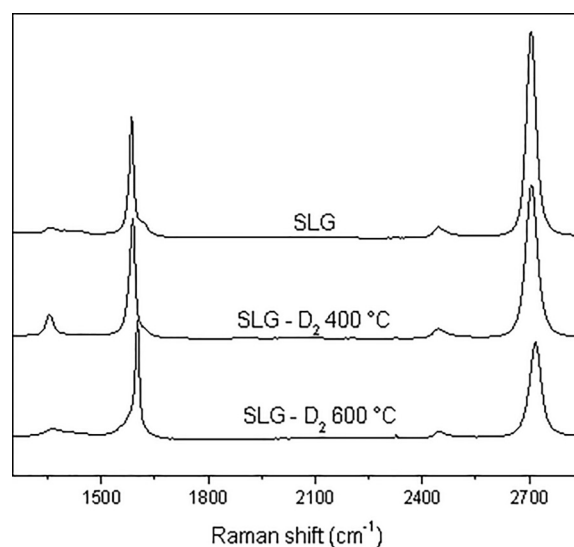
Figure 3 shows normalized C 1 s NEXAFS spectra obtained with an angle of incidence of (a) 26° and (b) 90° for a pristine sample (red line) and samples annealed in D_2 at 400 (blue line) and 600 °C (green line). Four main resonance peaks were observed: π*(C=C) at 285 eV, σ*(C—H) at 287 eV, σ*(C—O) at 288 eV, and σ*(C—C) at 291.3 eV.[26–28] Fig. 3(a) shows that the π* peak increases with D_2 annealing temperature in agreement with XPS data. This increase is related to a higher availability of π delocalized electrons.[24] This observation also evidences that hydrogen does not bond to the basal plane of the graphene, which would modify C hybridization and lower the amount of π delocalized electrons. Thus, hydrogen is most probably bonded to the grain boundaries of graphene. Another interesting effect of deuterium annealing was the increase of the σ* resonance at this angle of incidence (more
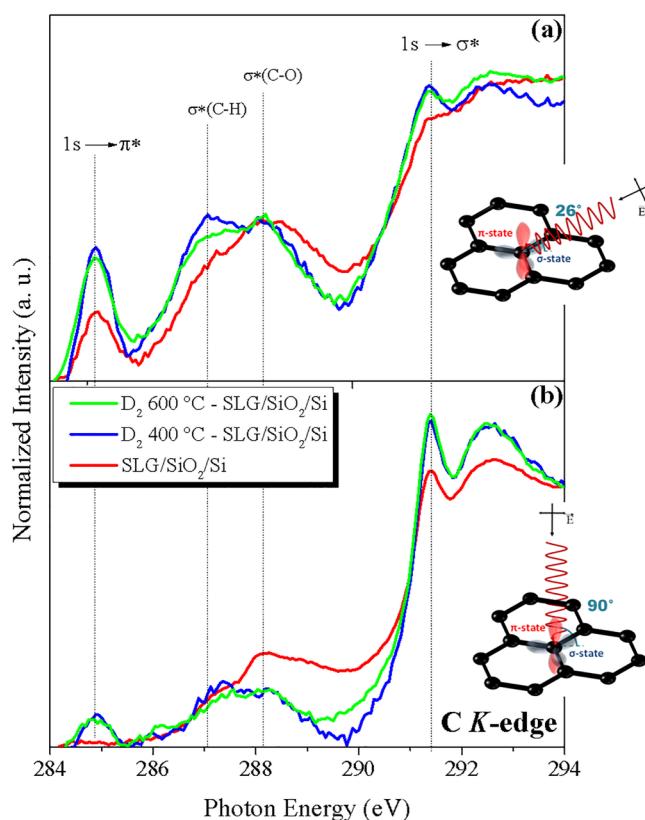
sensitive to bonds in the plane of the sample). This observation is probably due to a higher corrugation induced by deuterium incorporation. Sheka et al. showed that hydrogen incorporation in one side of graphene tends to roll up the sheet by hydrogen bonded either at the basal plane or at the edges of graphene.[29] Fig. 3(b) shows that the signal related to C—O bonding decreases with D_2 annealing in agreement with XPS data. The increase of the π* resonance is also observed, probably due to a higher corrugation of graphene. Moreover, comparing C—H signals (~287 eV) from deuterated samples measured at different angles of incidence, a higher intensity is observed for 26°. This observation suggests that the C—H bond is not parallel to the graphene basal plane.

Raman spectroscopy was used to access the structural quality and the defect density in graphene. Raman spectra of graphene samples exhibited D (~1350 cm^{-1}), G (~1590 cm^{-1}), and 2D (~2700 cm^{-1}) bands. The G band is related to linear vibration between pairs of carbon atoms bonded by sp^2 hybridization. The D band is related to the vibration movement of the hexagonal ring of graphene, and its intensity is related to the presence of defects in the graphene crystal. The 2D band is related to a process of second-order scattering and its intensity is associated with the quality of graphene. Figure 4 shows the spectra obtained for the pristine sample and those annealed in D_2 at 400 and 600 °C. The pristine sample shows a characteristic Raman spectrum of high-quality graphene, with a 2D peak with a higher intensity than that of G. Moreover, the D peak is almost undetectable. The sample annealed in D_2 at 400 °C shows a higher intensity of the D band, related to a higher defect density. Burgess et al. relate the intensity increase of this peak with the hydrogen incorporation.[17] We also observed a decrease in the intensity of the 2D peak with increasing annealing temperature. The spectrum of the sample treated at 600 °C in D_2 shows broadening of the D peak in addition to the asymmetry of the

FIG. 3. NEXAFS spectra of the carbon K-edge as a function of D_2 annealing temperature measured at (a) 26° and (b) 90° in relation to the sample plane. Dotted vertical lines mark the π*(C=C), σ*(C—H), σ*(C—O), and σ*(C=C) signals.

FIG. 4. Raman spectra of the pristine sample and those annealed in D_2.

G peak. These features are also observed in carbon nanotube spectra due to splitting of the G peak in G^- and G^+.[30] These results indicate that graphene is rippling due to D_2 annealing in agreement with NEXAFS data.

In order to verify the homogeneity of graphene, Raman mapping was performed. $12 \times 12 \, \mu m^2$ areas were scanned by a laser spot with a diameter of $1 \, \mu m$. Figure 5 shows Raman maps for the ratio between the areas of the 2D and G peaks for the pristine sample (a) and those annealed in D_2 at 400 (b), 600 (c), and 800 °C (d). This ratio is related to graphene quality: the higher the ratio, the higher the structural quality. The color scale is related to the A_{2D}/A_G ratio as indicated. The map of Fig. 5(a) was obtained from the pristine sample, evidencing the homogeneity and quality of this graphene layer. An A_{2D}/A_G ratio higher than 3 is observed in almost the entire area. Figure 5(b) shows that annealing in D_2 at 400 °C decreases the quality of graphene in specific regions, mainly on the right side of the image. An additional increase in the annealing temperature decreases the overall quality as seen in Fig. 5(c). Finally, annealing at 800 °C shows a large area, in the upper left corner, where no graphene signal was obtained, indicating etching of graphene at this temperature [Fig. 5(d)]. A direct consequence of this process is the higher density of grain boundaries that constitute new incorporation sites for D. This effect contributes to the increase in the D amount detected by NRA for higher annealing temperatures. In addition, the lower graphene quality of annealed samples is probably due to a thermal effect,[31] which generates defects in the structure of the remnant graphene.

Figure 6 shows Raman maps of the ratio between the areas of the D and G peaks for the pristine sample (a) and those annealed
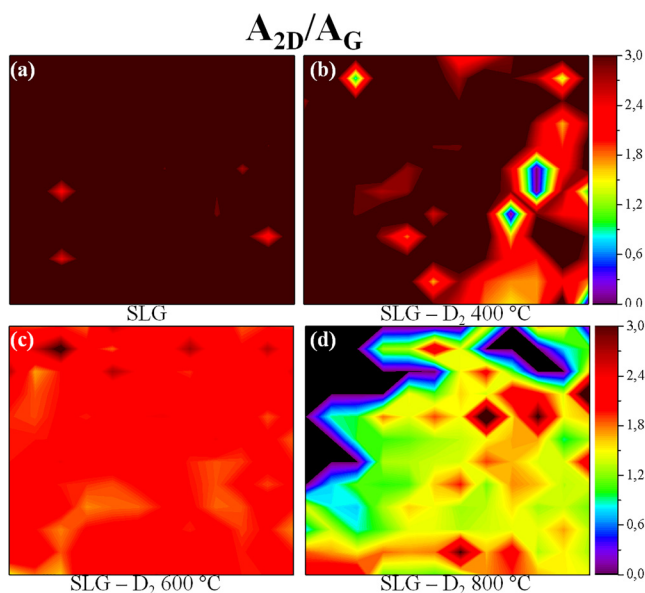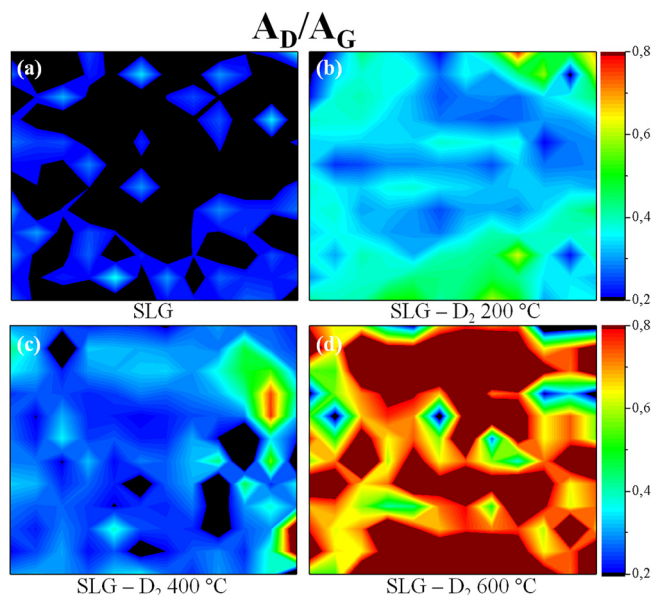
FIG. 6. Maps of the A_D/A_G Raman signal ratio obtained from (a) pristine samples and samples annealed under a D_2 atmosphere at (b) 200 °C, (c) 400 °C, and (d) 600 °C.

in D_2 at 200 (b), 400 (c), and 600 °C (d). This ratio is related to defects[32] and, eventually, to hydrogenation of graphene.[17] The color scale is related to the A_D/A_G ratio as indicated. Figure 6(a) shows that the pristine sample presents a ratio higher than 0.2 at specific regions. This observation is probably related to defects created during growth and transfer processes, as previously discussed. Defective regions are observed throughout the whole investigated area in Fig. 6(b), obtained from a sample following annealing in D_2 at 200 °C. Since the incorporated D amount was below the sensitivity of the NRA technique at this temperature, this result is probably due to defects generated by the thermal effect. No significant modification of this scenario is obtained following annealing at 400 °C [Fig. 6(c)]. However, following annealing at 600 °C [Fig. 6(d)], a higher A_D/A_G ratio is obtained throughout the sample as a result of both the thermal effect and D incorporation.

D desorption from graphene was investigated using samples annealed at 600 °C in D_2. Following the D_2 annealing step, samples were annealed in a N_2 atmosphere at different temperatures to verify the thermal stability of incorporated deuterium. Figure 7 shows D areal densities as a function of the N_2 annealing temperature. The areal density obtained from a sample following annealing in D_2 at 600 °C is also plotted for comparison (a value of 0 °C was attributed as its abscissa). Up to 400 °C, no significant deuterium desorption is observed. Following annealing at 600 °C, lower D areal densities are observed for both samples (with and without graphene). However, the difference between these values has no prominent variation compared with lower annealing temperatures. This result indicates that D incorporated in graphene is stable up to 600 °C and that D (at this temperature) desorbs predominantly
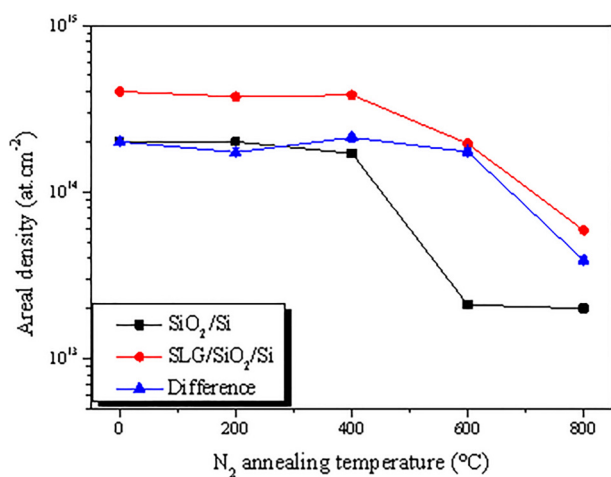

FIG. 5. Maps of the A_{2D}/A_G Raman signal ratio obtained from pristine and deuterium annealed samples. (a) SLG. Samples annealed under a D_2 atmosphere at (b) 400 °C, (c) 600 °C, and (d) 800 °C.

FIG. 7. D areal densities as a function of N_2 annealing temperature for 285 nm thick SiO_2 films grown on Si (black squares) and single-layer graphene transferred to 285 nm thick SiO_2 films grown on Si (red circles). Samples were previously annealed in D_2 at 600 °C. The point at 0 °C corresponds to the sample without N_2 annealing. The difference between D areal densities in samples with and without graphene is represented by blue triangles. Lines are only to guide the eyes.

FIG. 8. Raman spectra of samples annealed in D_2 and those following an additional N_2 annealing step.

from the SiO_2/Si substrate. At 800 °C, the difference in areal densities reaches ~20% of its initial value, evidencing that D desorption from graphene takes place in this upper limit.

Several authors investigated the reversibility of the hydrogenation process.[33,34] Raman spectroscopy is the most used technique to verify the effects of a hydrogen adsorption–desorption cycle in the graphene structure. Figure 8 shows spectra obtained from (i) a sample annealed in D_2 at 600 °C and samples (following the same annealing in D_2) with an additional annealing step in N_2 at (ii) 600 and (iii) 800 °C. The sample annealed in deuterium shows broad D and asymmetric G signals, like a spectrum obtained from carbon nanotubes. Following annealing at 600 °C in N_2, no prominent modifications are observed. This result agrees with NRA data that show that D is not desorbed from graphene at this temperature. However, the sample treated at 800 °C under a N_2 atmosphere presents a Raman spectrum quite distinct from the previous ones: a prominent D peak is observed and the G peak splits. Moreover, we observe a slight increase in the intensity of the 2D peak, similar to those observed for samples annealed at lower temperatures in D_2.

Figure 9 shows Raman maps of the ratio between the areas of the D and G peaks for the sample annealed in D_2 at 600 °C (a) and samples (following the same annealing in D_2) with an additional annealing step in N_2 at 400 (b), 600 (c), and 800 °C (d). Figures 9(b) and 9(c) show that N_2 annealing does not modify the density of defects in the graphene structure, at least in this temperature range. In contrast to this behavior, the sample annealed at 800 °C [Fig. 9(d)] shows a lower A_D/A_G ratio. It is worth mentioning that D desorption from graphene was observed at this temperature by NRA. Despite not returning to the original value of the
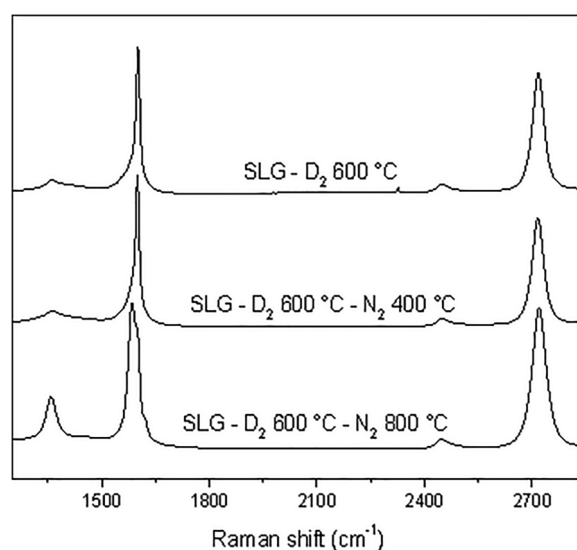
pristine sample, the lowering of the A_D/A_G ratio evidences a certain degree of reversibility of the graphene hydrogenation process. Etching of graphene is a parallel effect of this cycling process, which certainly accounts for its reduced reversibility.
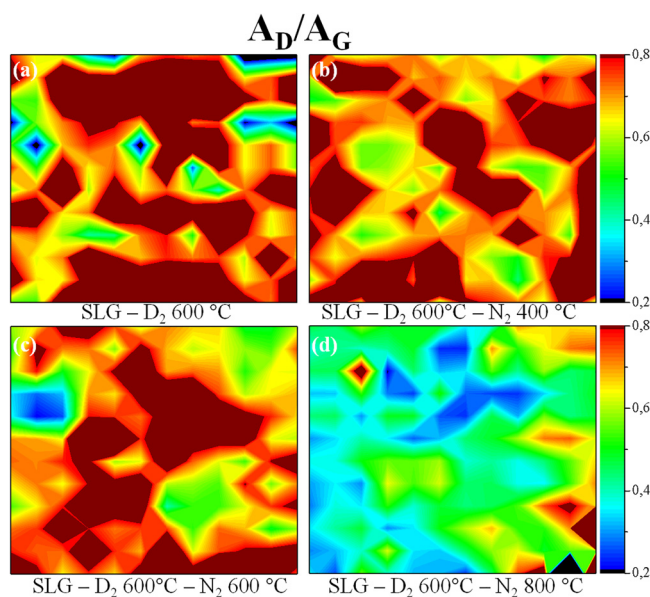
FIG. 9. Maps of the A_D/A_G Raman signal ratio obtained from samples (a) SLG annealed in a D_2 atmosphere at 600 °C and samples annealed in N_2 after D_2 at (b) 400 °C, (c) 600 °C, and (d) 800 °C.

CONCLUSION

In summary, we investigated the thermally driven hydrogen incorporation in monolayer graphene on SiO_2/Si by isotopic labeling. We used an isotopically enriched atmosphere in deuterium to quantify the amount of this isotope that is incorporated specifically during annealing. Using this technique, we circumvented experimental hurdles of hydrogen quantification usually experienced, such as incorporation of hydrogenated contaminants on the sample surface. We showed that D incorporation in graphene takes place above 400 °C. Above this limit, the amount incorporated increases until 800 °C. At this temperature, a D areal density of 3.5×10^{14} D/cm^2 was obtained, corresponding to ~10% of carbon atoms in graphene. Desorption experiments performed in N_2 atmosphere evidenced that D incorporated in graphene by thermal annealing is stable: until 600 °C, the D amount remained almost constant. Spectroscopic results evidence that D is predominantly incorporated in grain boundaries accompanied by rippling and etching of graphene, the latter effect being more pronounced at higher temperatures. This result has consequences in the reversibility of the hydrogenation process. The damage induced in the graphene layer through the hydrogen adsorption/desorption cycle limits the use of this method for hydrogen storage. Nevertheless, the observed thermal stability of hydrogenated graphene paves the way for its use as a material in electronic devices.

ACKNOWLEDGMENTS

DATA AVAILABILITY

The data that support the findings of this study are available from the corresponding author upon reasonable request.

REFERENCES

[1]A. K. Geim and K. S. Novoselov, "The rise of graphene," Nat. Mater. **6**, 183–191 (2007).

[2]N. Savage, "Materials science: Super carbon," Nature **483**, S30–S31 (2012).

[3]A. C. Ferrari et al., "Science and technology roadmap for graphene, related two dimensional crystals, and hybrid systems," Nanoscale **7**, 4598–4810 (2015).

[4]L. Colombo et al., "Graphene growth and device integration," Proc. IEEE **101**, 1536–1556 (2013).

[5]G. R. Yazdi et al., "Growth of large area monolayer graphene on 3C-SiC and a comparison with other SiC polytypes," Carbon **57**, 477–484 (2013).

[6]J. M. Garcia et al., "Graphene growth on h-BN by molecular beam epitaxy," Solid State Commun. **152**, 975–978 (2012).

[7]S. Bae et al., "Roll-to-roll production of 30-inch graphene films for transparent electrodes," Nat. Nanotechnol. **5**, 574–578 (2010).

[8]Y. M. Lin, C. Dimitrakopoulos, K. A. Jenkis, D. B. Farmer, H. Y. Chiu, A. Grill, and P. Avouris, "100 GHz transistors from wafer scale epitaxial graphene," Science **327**, 662 (2010).

[9]Z. H. Ni et al., "The effect of vacuum annealing on graphene," J. Raman Spectrosc. **41**, 479–483 (2010).

[10]O. V. Yazyev et al., "Defect-induced magnetism in graphene," Phys. Rev. B **75**, 125408 (2007).

[11]J. O. Sofo et al., "Graphane: A two-dimensional hydrocarbon," Phys. Rev. B **75**, 153401 (2007).

[12]G. Fiori, "Simulation of hydrogenated graphene field-effect transistors through a multiscale approach," Phys. Rev. B **82**, 153404 (2010).

[13]G. K. Dimitrakakis et al., "Pillared graphene: A new 3-D network nanostructure for enhanced hydrogen storage," Nano Lett. **8**, 3166–3170 (2008).

[14]Y. S. Nechaev, "On the solid hydrogen carrier intercalation in graphane-like regions in carbon-based nanostructures," Int. J. Hydrog. Energy **36**, 9023–9031 (2011).

[15]T. Hussain et al., "Polylithiated (OLi$_2$) functionalized graphane as a potential hydrogen storage material," Appl. Phys. Lett. **101**, 243902 (2012).

[16]Z. Luo et al., "Modulating the electronic structures of graphene by controllable hydrogenation," Appl. Phys. Lett. **97**, 233111 (2010).

[17]J. S. Burgess et al., "Tuning the electronic properties of graphene by hydrogenation in a plasma enhanced chemical vapor deposition reactor," Carbon **49**, 4420 (2011).

[18]S. M. Myers, "Interaction of deuterium gas with dry SiO_2 on Si: An ion-beam study," J. Appl. Phys. **61**, 5428 (1987).

[19]M. S. Fuhrer et al., "Graphene: Materially better carbon," MRS Bull. **35**, 289–295 (2010).

[20]S. Wang et al., "Raman spectroscopic investigation of polycrystalline structures of CVD-grown graphene by isotope labeling," Nanoscale **6**, 13838 (2014).

[21]W. Xie et al., "Clean graphene surface through high annealing temperature," Carbon **94**, 740–748 (2015).

[22]Y. Ahn et al., "Procedure of removing polymer residues and its influences on electronic and structural characteristics of graphene," Appl. Phys. Lett. **102**, 091602 (2013).

[23]S. S. Roy et al., "Evolution, kinetics, energetics, and environmental factors of graphene degradation on silicon dioxide," Nanoscale **7**, 6093 (2015).

[24]I. Retzko et al., "Analysis of carbon materials by x-ray photoelectron spectroscopy and x-ray absorption spectroscopy," Adv. Eng. Mater. **5**, 519 (2003).

[25]K. Dave et al., "Two-step process for programmable removal of oxygen functionalities of graphene oxide: Functional, structural and electrical characteristics," RSC Adv. **5**, 95657 (2015).

[26]G. Hähner, "Near edge x-ray absorption fine structure spectroscopy as a tool to probe electronic and structural properties of thin organic film and liquids," Chem. Soc. Rev. **35**, 1244–1255 (2006).

[27]V. Lee et al., "Substrate hybridization and rippling of graphene evidenced by near-edge x-ray absorption fine structure spectroscopy," J. Phys. Chem. Lett. **1**, 1247 (2010).

[28]V. Lee et al., "Large-area chemically modified graphene films: Electrophoretic deposition and characterization by soft x-ray absorption spectroscopy," Chem. Mater. **21**, 3905 (2009).

[29]E. F. Sheka et al., "Odd-electron molecular theory of graphene hydrogenation," J. Mol. Model. **18**, 3751 (2012).

[30]R. Saito et al., "Raman spectroscopy of graphene and carbon nanotubes," Adv. Phys. **60**, 413 (2011).

[31]N. M. Bom et al., "Water incorporation in graphene transferred onto SiO_2/Si investigated by isotopic labeling," J. Phys. Chem. C **120**, 201 (2016).

[32]A. C. Ferrari et al., "Raman spectroscopy as a versatile tool for studying the properties of graphene," Nat. Nanotechnol. **8**, 235 (2013).

[33]S. Ryu et al., "Reversible basal plane hydrogenation of graphene," Nano Lett. **8**, 4597 (2008).

[34]D. C. Elias et al., "Control of graphene's properties by reversible hydrogenation: Evidence for graphane," Science **323**, 610 (2009).